

On the Computation of Intrinsic Volumes

Daniel Meschenmoser
Institute of Stochastics
Ulm University
89069 Ulm
Germany

daniel.meschenmoser@uni-ulm.de

Evgeny Spodarev
Institute of Stochastics
Ulm University
89069 Ulm
Germany

evgeny.spodarev@uni-ulm.de

December 14, 2010

Abstract

Many methods are known to compute the intrinsic volumes of a set given in a digital image. However, most of these methods have the disadvantage that they are not multigrid convergent. This means that the computed values do not converge to the true values for increasing resolution of the digital image. One exception is the volume which can easily be estimated by counting pixels and the Euler characteristic for which Kiderlen [14] presented a multigrid convergent estimator for polyconvex sets with some regularity assumptions. We propose two methods for the computation of all $d+1$ intrinsic volumes which are multigrid convergent for \mathcal{U}_{PR} -sets under mild regularity assumptions. The \mathcal{U}_{PR} -class contains sets which can be represented as a finite union of compact sets with positive reach and include polyconvex sets. We provide numerical results and compare this approach with other methods known in the literature.

2010 Mathematics Subject Classification: Primary [65D18](#); Secondary [68U05](#), [52A38](#)

Keywords and phrases: intrinsic volumes, Minkowski functionals, multigrid convergence, polyconvex sets, positive reach, Wills functional

1 Introduction

The intrinsic volumes are functionals which describe the global characteristics of a set, for example volume, surface area or Euler characteristic. They are used in various contexts,

for example in medicine to classify tissues (see [3]), in cosmology to characterize the galaxy distribution (see [13]) or in material science to analyse foams and other porous media (see [9] and [22]).

In the literature, various methods are known to compute the intrinsic volumes of a polyconvex set from a digital image. For example, the method in [20] is based on a discretized Crofton formula while the approach in [24] is based on the principal kinematic formula. In [19] an asymptotically unbiased estimator for the intrinsic volume densities of a stationary random closed set Ξ is presented and numerical results are given for Boolean models in the plane. The surface area of a three-dimensional stationary and isotropic Boolean model is estimated in an asymptotically unbiased way in [21]. Attempts have also been made to estimate tensor-valued Minkowski functionals, see [2] for an introduction into the subject as well as numerical results. However, most of the methods to compute the intrinsic volumes have in common that they are not convergent, see e.g. [15] for error bounds and an improvement of the method in [20]. To make the term “convergence” more precise we define the notion of *multigrid convergence* following [18]. Let \mathcal{M} be a family of sets in \mathbb{R}^d and let $\{K^n\}$ be a sequence of discretizations of $K \in \mathcal{M}$ on grids with mesh size $t_n \searrow 0, n \rightarrow \infty$. Let ϕ be some real valued functional defined on \mathcal{M} . An estimator (functional) $\hat{\phi} : \mathcal{M} \rightarrow \mathbb{R}$ is called multigrid convergent to ϕ for the class \mathcal{M} and the chosen digitization model if

$$\lim_{n \rightarrow \infty} \hat{\phi}(K^n) = \phi(K), \quad K \in \mathcal{M}.$$

Already C.F. Gauss, the *Princeps mathematicorum*, knew that the area of a disc can be estimated multigrid convergently by counting the points of a square grid which lie inside this disc, see [7, pp. 269–291]. But this is not only true for discs. It is well-known that the intuitive approach of pixel counting yields a multigrid convergent estimator for the volume. Hence we focus on estimating the lower dimensional intrinsic volumes as for these it is not obvious how they can be estimated multigrid convergently for a rich family of sets.

There are algorithms in the literature which are proven to be multigrid convergent for some of the Minkowski functionals for a class of sets satisfying some restrictive conditions. For the surface area there is an approach by Coeurjolly et al. in [4]. It is based on the estimation of surface normals and discrete integration of the surface normal vector field. They prove multigrid convergence for Jordan surfaces in \mathbb{R}^3 with continuous derivatives. Recently, Kiderlen [14] proposed a multigrid convergent estimator of the Euler number for two-dimensional polyconvex sets with some regularity assumptions and the Gauss digitization. He also detected an error in [16]. There it was claimed in Section 4.4 that the conditions which ensure multigrid convergence are fulfilled for any two-dimensional convex set K without lower dimensional parts. For example, the triangle in Figure 1 has no lower dimensional parts but it does not fulfil these conditions because the digitization consists of two separated objects for any grid resolution.

We shall choose the family of finite unions of compact sets with positive reach for \mathcal{M} and denote this class by \mathcal{U}_{PR} . We suggest a modification of the method in [16] to estimate all $d+1$ intrinsic volumes multigrid convergently. It is based on a generalization

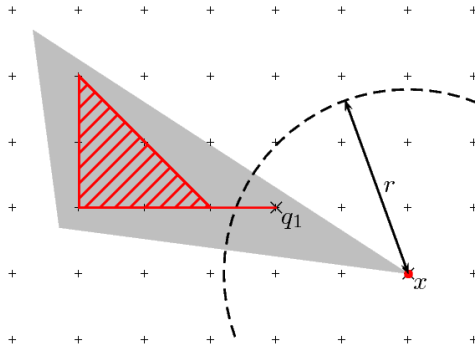


Figure 1: Counterexample to the statement in Section 4.4 of [16]. In their notation, K is the solid gray triangle and $K_{\mathbb{F}(G_{\max})}$ is shaded in red. Hence, $I_r(K_{\mathbb{F}(G_{\max})}, x) = J(K_{\mathbb{F}(G_{\max})} \cap B_r(x), q_1, x) = 1 \neq 0$ which means that the method in [16] is not multigrad convergent for any convex body without lower dimensional parts.

of Wills functional and a polygonal approximation with arbitrarily large polygons, i.e. it is not a local approach based on pixel configurations.

The paper is organized as follows. First, we shortly recall some basic definitions in Section 2. Then we prove the main result in Theorem 2, which shows that, if a \mathcal{U}_{PR} -set K is approximated by \mathcal{U}_{PR} -sets K^n in a suitable way, the intrinsic volumes $V_j(K^n)$ converge to the intrinsic volumes $V_j(K)$. In the last part of Section 2, we propose a method to compute the intrinsic volumes which is based on a generalization of Wills functional and Theorem 2. In Section 3 we give details on how to find an approximation of the unknown set K if only a digital image of K is known. The section is split into three parts dealing with polyconvex sets, sets with positive reach, and \mathcal{U}_{PR} -sets, respectively. In Section 4 we provide various test cases as well as numerical results and a comparison with other methods.

2 Intrinsic volumes and their approximation

It is well known (see e.g. [23]) that there exist non-negative functionals V_0, \dots, V_d , called *intrinsic volumes*, on the family of d -dimensional convex bodies (i.e. non-empty compact convex sets) which satisfy *Steiner's formula*

$$V_d(K \oplus B_r(o)) = \sum_{j=0}^d r^{d-j} \kappa_{d-j} V_j(K), \quad r > 0 \quad (1)$$

where V_d denotes the Lebesgue measure, $B_r(o)$ is the ball of radius r centered at the origin o and κ_j is the volume of the unit ball in \mathbb{R}^j . These functionals can be extended

additively in a unique way to *polyconvex sets*, i.e. finite unions of convex bodies via the *inclusion-exclusion-formula*

$$V_j \left(\bigcup_{i=1}^m K_i \right) = \sum_{k=1}^m (-1)^{k+1} \sum_{1 \leq i_1 < \dots < i_k \leq m} V_j (K_{i_1} \cap \dots \cap K_{i_k}) \quad (2)$$

for any $j = 0, \dots, d$ and for any convex bodies K_1, \dots, K_m . Some of these functionals have a nice geometric interpretation. V_d is the usual d -dimensional volume, $2V_{d-1}$ is the surface area, and V_0 is the Euler characteristic which describes the porosity of a set. The intrinsic volumes are closely related to the *Minkowski functionals* W_j by the relation

$$W_j (K) = \frac{\kappa_j}{\binom{d}{j}} V_{d-j}$$

for $j = 0, \dots, d$.

The *reach* of a compact subset K of \mathbb{R}^d , denoted by $\text{reach}(K)$, is the largest ε such that all points in an ε -neighbourhood of K have a unique metric projection in K . A set K has *positive reach* if $\text{reach}(K) > 0$. See [6] for details on sets with positive reach and Figure 2 for examples. *Convex bodies* can be characterized as sets with infinite reach and are, as well as polyconvex sets, included in the family \mathcal{U}_{PR} of finite unions of compact sets with positive reach. The intrinsic volumes are well-defined for sets with positive

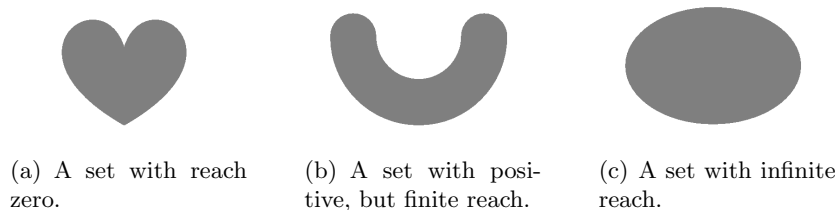


Figure 2: Examples for sets with reach zero, positive and infinite reach, respectively.

reach and Steiner's formula (1) does also hold under the restriction that $r < \text{reach}(K)$. The inclusion-exclusion-formula (2) is also true for \mathcal{U}_{PR} -sets.

The *Hausdorff distance* ρ of two nonempty compact sets A and B is defined as

$$\rho(A, B) = \inf \{ \alpha \geq 0 : A \subset B \oplus B_\alpha(o) \text{ and } B \subset A \oplus B_\alpha(o) \}.$$

Denote the Euclidean distance between two points $x, y \in \mathbb{R}^d$ by $d(x, y)$ and the distance between a point x and a compact set $A \subset \mathbb{R}^d$ by $d(x, A) = \inf \{ d(x, a) : a \in A \}$. Then it holds that

$$\rho(A, B) = \sup_{x \in \mathbb{R}^d} |d(x, A) - d(x, B)| \quad (3)$$

for compacts $A, B \subset \mathbb{R}^d$, see [5, Remark 4.14].

2.1 Multigrid convergent computation of the intrinsic volumes based on the inclusion-exclusion-formula

In this section we show how multigrid convergence can be achieved for the computation of the intrinsic volumes via the inclusion-exclusion-formula (2). The following lemma is needed for the proof of Theorem 2.

Lemma 1. *Let $K_1, \dots, K_m \subset \mathbb{R}^d$ be compact sets. Let $\{K_i^n\}_{n \in \mathbb{N}}$ be a sequence of compact approximations converging to K_i in Hausdorff distance, such that $K_i \subset K_i^n$ for all $n \in \mathbb{N}$ and for $i = 1, \dots, m$. Then it holds that*

$$\rho \left(\bigcap_{i=1}^m K_i^n, \bigcap_{i=1}^m K_i \right) \rightarrow 0, \quad n \rightarrow \infty.$$

The present short proof (due to J. Kampf, personal communication) is more elegant than the original proof by the authors.

Proof. Assume that $\bigcap_{i=1}^m K_i^n$ does not converge to $\bigcap_{i=1}^m K_i$. Then there is an $\varepsilon > 0$ such that

$$\rho \left(\bigcap_{i=1}^m K_i^n, \bigcap_{i=1}^m K_i \right) > \varepsilon$$

for all n large enough. Furthermore, there is a ball $B_s(o)$ such that $\bigcap_{i=1}^m K_i^n \subset B_s(o)$ for all n . By Blaschke's selection theorem (see Theorem 12.3.3 in [23]), there exists a sequence $\{n_k\}$ with $n_k \rightarrow \infty$ as $k \rightarrow \infty$ such that $\bigcap_{i=1}^m K_i^{n_k}$ converges towards a limit set L for $k \rightarrow \infty$. This implies that $\rho(L, \bigcap_{i=1}^m K_i^{n_k}) > \varepsilon$ for sufficiently large k . From $\bigcap_{i=1}^m K_i \subset \bigcap_{i=1}^m K_i^{n_k}$ it follows that $\bigcap_{i=1}^m K_i \subset L$ but $\bigcap_{i=1}^m K_i \neq L$. Then there exists a point $x \in L \setminus \bigcap_{i=1}^m K_i$. In particular, there is a $j \in \{1, \dots, m\}$ with $x \notin K_j$ and therefore there exists a $\delta > 0$ with $x \notin K_j \oplus B_\delta(o)$. Hence, $x \notin K_j^{n_k} \oplus B_{\delta/2}(o)$ and $x \notin (\bigcap_{i=1}^m K_i^{n_k}) \oplus B_{\delta/2}(o)$ for all k large enough. This means that $x \notin L$. We arrived at a contradiction. \square

The following theorem ensures the convergence of the intrinsic volumes of an \mathcal{U}_{PR} -approximation K^n of an \mathcal{U}_{PR} -set K towards the intrinsic volumes of the original set K whenever the approximation K^n converges to K in Hausdorff distance. No conditions like “no-touching” or “no lower dimensional parts” are required and the convergence is guaranteed not only for polyconvex sets but also for \mathcal{U}_{PR} -sets.

Theorem 2. *Let $K = \bigcup_{i=1}^m K_i \subset \mathbb{R}^d$ be a \mathcal{U}_{PR} -set consisting of sets K_i with positive reach. Let $\{K^n\}_{n \in \mathbb{N}}$ with $K^n = \bigcup_{i=1}^m K_i^n \subset \mathbb{R}^d$ be a sequence of \mathcal{U}_{PR} -approximations of K such that the following three conditions are fulfilled:*

- $\min_{i=1, \dots, m} \inf_{n \in \mathbb{N}} \text{reach}(K_i^n) > 0$
- $K_i \subset K_i^n$ for all $i = 1, \dots, m$ and all $n \in \mathbb{N}$
- $\rho(K_i^n, K_i) \rightarrow 0$ as $n \rightarrow \infty$ for all $i = 1, \dots, m$

Then it holds that

$$V_j(K^n) \rightarrow V_j(K), \quad n \rightarrow \infty \quad (4)$$

for all $j = 0, \dots, d$.

Proof. By the inclusion-exclusion-formula it holds that

$$V_j(K^n) = \sum_{i=1}^m (-1)^{i+1} \sum_{1 \leq k_1 < \dots < k_i \leq m} V_j(K_{k_1}^n \cap \dots \cap K_{k_i}^n). \quad (5)$$

Lemma 1 implies that

$$\rho(K_{k_1}^n \cap \dots \cap K_{k_i}^n, K_{k_1} \cap \dots \cap K_{k_i}) \rightarrow 0 \text{ as } n \rightarrow \infty.$$

By (3), this is equivalent to

$$d(x, K_{k_1}^n \cap \dots \cap K_{k_i}^n) \rightarrow d(x, K_{k_1} \cap \dots \cap K_{k_i})$$

uniformly for all $x \in \mathbb{R}^d$. Furthermore, it holds that

$$\text{reach}(K_{k_1}^n \cap \dots \cap K_{k_i}^n) \geq \varepsilon = \min_{i=1, \dots, m} \inf_{n \in \mathbb{N}} \text{reach}(K_i^n).$$

Theorem 5.9 in [5] implies that $\varepsilon \leq \text{reach}(K_{k_1} \cap \dots \cap K_{k_i})$ and that

$$V_j(K_{k_1}^n \cap \dots \cap K_{k_i}^n) \rightarrow V_j(K_{k_1} \cap \dots \cap K_{k_i}) \quad (6)$$

as $n \rightarrow \infty$. Therefore the convergence in (4) follows from (5) and (6). \square

Now that the theoretical foundations are laid, a practical problem is how to find a suitable approximation K^n of K and how to compute the intrinsic volumes $V_j(K^n)$. The latter question is answered in the next subsection with an approach based on Wills-type functionals. The first question is postponed to Section 3.

2.2 Multigrid convergent computation of the intrinsic volumes based on Wills-type functionals

For convex bodies K , *Wills functional* $W(K)$ (first introduced in [26]) is defined by

$$W(K) = \sum_{j=0}^d V_j(K).$$

It can be written as an integral

$$W(K) = \int_{\mathbb{R}^d} \exp(-\pi d(x, K)^2) dx. \quad (7)$$

As Vitale showed in [25], equation (7) can be proved easily with the help of Steiner's formula.

On the right hand side of equation (7), the integrand is the tail function of a Weibull-distributed random variable with parameters $(2, \pi)$. One possibility to generalise this formula is to allow for other distributions. Let \overline{F} denote the tail function of some random variable ξ with $\mathbb{E}\xi^d < \infty$. For any convex body K it holds that

$$\int_{\mathbb{R}^d} \overline{F}(d(x, K)) dx = \sum_{j=0}^d \mathbb{E}\xi^{d-j} \kappa_{d-j} V_j(K).$$

Another generalisation was given recently by Kampf in [11]. For any convex body K and any integrable function $G : [0, \infty) \rightarrow \mathbb{R}$ with $y \mapsto y^{d-1}G(y)$ integrable, it holds that

$$\int_{\mathbb{R}^d} G(d(x, K)) dx = \sum_{j=0}^d c_j V_j(K) \quad (8)$$

where the coefficients c_j , $j = 0, \dots, d$, are given by

$$c_j = \begin{cases} (d-j) \kappa_{d-j} \int_0^\infty x^{d-j-1} G(x) dx & j = 0, \dots, d-1, \\ G(0) & j = d. \end{cases}$$

If $K = \bigcup_{i=1}^m K_i$ is a \mathcal{U}_{PR} -set and the support of the function G is a subset of the interval $\left[0, \min_{i=1, \dots, m} \text{reach}(K_i)\right)$, we get by the inclusion-exclusion formula (2) and equation (8) that

$$\sum_{j=0}^d c_j V_j(K) = \sum_{k=1}^m (-1)^{k+1} \sum_{1 \leq i_1 < \dots < i_k \leq m} \int_{\mathbb{R}^d} G(d(x, K_{i_1} \cap \dots \cap K_{i_k})) dx.$$

As Guderlei et al. point out in [8], Hadwiger's characterization theorem can be applied to $d+1$ functionals F_0, \dots, F_d to obtain a system of $d+1$ linear equations of the type

$$F_i(K) = \sum_{j=0}^d \alpha_{ij} V_j(K), \quad i = 0, \dots, d \quad (9)$$

for any convex body K with coefficients $\alpha_{ij} \in \mathbb{R}$ depending on the functional F_i . The generalisation to \mathcal{U}_{PR} -sets by the inclusion-exclusion-formula is straightforward. If the functionals F_0, \dots, F_d are chosen in such a way that the matrix $(\alpha_{ij})_{i,j=0, \dots, d}$ is invertible, we can get the intrinsic volumes of K as the solution of (9).

We use this idea together with the generalized Wills functional to construct a multi-grid convergent estimator for the intrinsic volumes under conditions which are slightly different from those in Theorem 2. Namely, it is not any longer required that $K_i \subset K_i^n$ for all $i = 1, \dots, m$ and all $n \in \mathbb{N}$. But on the other hand, the function G in (8) has to fulfill certain conditions. The differences between Theorem 2 and Proposition 3 lead to different error rates as can be seen from the examples in Section 4.

Proposition 3. Let $K = \bigcup_{i=1}^m K_i \subset \mathbb{R}^d$ be a \mathcal{U}_{PR} -set consisting of sets K_i with positive reach. Let $\{K^n\}_{n \in \mathbb{N}}$ with $K^n = \bigcup_{i=1}^m K_i^n \subset \mathbb{R}^d$ be a sequence of \mathcal{U}_{PR} -approximations of K such that the following two conditions are fulfilled:

- $r = \min_{i=1, \dots, m} \left\{ \inf_{n \in \mathbb{N}} \text{reach}(K_i^n), \text{reach}(K_i) \right\} > 0$
- $\rho(K_i^n, K_i) \rightarrow 0$ as $n \rightarrow \infty$ for all $i = 1, \dots, m$.

Let $G : [0, \infty) \rightarrow \mathbb{R}$ be a continuous function with compact $\text{supp}(G) \subset [0, r)$. Then it holds that

$$\lim_{n \rightarrow \infty} \int_{\mathbb{R}^d} G(d(x, K^n)) dx = \int_{\mathbb{R}^d} G(d(x, K)) dx. \quad (10)$$

Proof. As $\rho(K_i^n, K_i) \rightarrow 0$ for all $i = 1, \dots, m$, we have $\rho(K^n, K) \rightarrow 0$ by [23, Theorem 12.3.5]. By (3), this implies that $d(x, K^n) \rightarrow d(x, K)$ uniformly in x . The continuity of G implies that $G(d(x, K^n)) \rightarrow G(d(x, K))$ for all $x \in \mathbb{R}^d$. As G is continuous and $\text{supp}(G) \subset [0, a]$ for some $a < r$, G is bounded, i.e. there exists a constant $c_0 > 0$ with $|G(y)| \leq c_0$ for all $y \in [0, \infty)$. The compactness of K and K^n and $\rho(K^n, K) \rightarrow 0$ imply that there exists a $c > 0$ such that $K, K^n \subset B_c(o)$ for all $n \in \mathbb{N}$. Hence, $\text{supp}(G(d(\cdot, K))) \subset B_{c+a}(o)$, $\text{supp}(G(d(\cdot, K^n))) \subset B_{c+a}(o)$ and

$$\left| \int_{\mathbb{R}^d} G(d(x, K^n)) dx \right| \leq \int_{B_{c+a}(o)} |G(d(x, K^n))| dx \leq c_0 V_d(B_{c+a}(o))$$

for all $n \in \mathbb{N}$. By Lebesgue's theorem, the limit and the integration in (10) can be interchanged and the proof is complete. \square

Under the conditions of Proposition 3, for $d+1$ pairwise different numbers $r_0, \dots, r_d > 0$ we get the following system of linear equations:

$$\lim_{n \rightarrow \infty} \begin{pmatrix} \sum_{k=1}^m (-1)^{k+1} \sum_{1 \leq i_1 < \dots < i_k \leq m} \int_{\mathbb{R}^d} G(r_0 d(x, K_{i_1}^n \cap \dots \cap K_{i_k}^n)) dx \\ \vdots \\ \sum_{k=1}^m (-1)^{k+1} \sum_{1 \leq i_1 < \dots < i_k \leq m} \int_{\mathbb{R}^d} G(r_d d(x, K_{i_1}^n \cap \dots \cap K_{i_k}^n)) dx \end{pmatrix} = \begin{pmatrix} r_0^{-d} c_0 & \dots & r_0^0 c_d \\ \vdots & & \vdots \\ r_d^{-d} c_0 & \dots & r_d^0 c_d \end{pmatrix} \begin{pmatrix} V_0(K) \\ \vdots \\ V_d(K) \end{pmatrix} \quad (11)$$

Since the numbers r_0, \dots, r_d are chosen pairwise different, the matrix of coefficients $(r_i^{j-d} c_j)_{i,j=0, \dots, d}$ is regular and (11) can be solved easily to yield the vector of intrinsic volumes. Hence we can compute the intrinsic volumes $V_j(K)$ if we can compute the integrals on the left side of (11) exactly. Therefore the function G and the approximating sequence K^n have to be chosen in a suitable way such that the above conditions on G

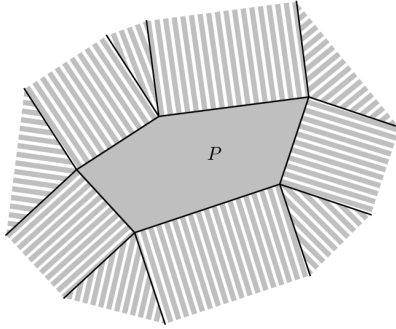


Figure 3: Partition of the Euclidean plane with respect to a given polygon P .

and K^n are fulfilled. For example, we can choose the piecewise linear function $G(x) = (b - ax) \mathbf{1}_{[0, b/a]}(x)$ for some $a, b > 0$ such that

$$b/a < r = \min_{i=1, \dots, m} \left\{ \inf_{n \in \mathbb{N}} \text{reach}(K_i^n), \text{reach}(K_i) \right\}.$$

It fulfills the conditions of Proposition 3. If the approximating sets K_i^n are polytopes, the sets $K_{i_1}^n \cap \dots \cap K_{i_k}^n$ appearing in the left hand side of (11) are also polytopes. Hence, each integral in the left hand side of (11) can be computed by partitioning the domain of integration as follows. Let $F_j(P)$ denote the set of j -dimensional faces of a polytope P and $\pi(x)$ the metric projection of a point $x \in \mathbb{R}^d$ onto P . Then, for any $j \in \{0, \dots, d\}$, it holds that

$$\int_{\mathbb{R}^d} G(r_j d(x, P)) dx = \sum_{i=0}^d \sum_{F \in F_i(P)} \int_{\pi^{-1}(\text{relint}(F))} G(r_j d(x, P)) dx, \quad (12)$$

where $\text{relint}(F)$ denotes the relative interior of the face F , i.e. the interior of F with respect to its affine hull. Figure 3 gives a sketch of the situation in the plane. The integrals on the right hand side of (12) can be computed easily by computing the (j -dimensional) volume of the faces and changing to spherical coordinates if necessary. The details on how to choose the approximation K^n appropriately are given in the next section.

3 How to approximate the set K

In view of Theorem 2 and Proposition 3, a practical problem is to find a sequence of \mathcal{U}_{PR} -sets K^n approximating the set K and satisfying the conditions of Theorem 2 and Proposition 3, respectively. This will be addressed for polyconvex sets in Section 3.1, for sets with positive reach in Section 3.2, and for general \mathcal{U}_{PR} -sets in Section 3.3, respectively. Throughout this section, we consider the case $d = 2$.

Generally, methods for the computation of intrinsic volumes can be divided into two classes. If the approximation K^n is given by a union of small construction bricks, e.g. all 0- to d -dimensional facets of cubes of fixed size or circles of fixed size, it is called a *local approach*, see for example the approach by Ohser and Mücklich in [20]. If this is not the case we speak of a *global approach*. The conditions in Theorem 2 are certainly not fulfilled for a local approach. In that case the number m of components K_i^n would grow to infinity as n grows which is a contradiction to the assumption that the number of components in K equals the number of components in the approximation for each step. Therefore we need a global approach which will be presented in the following.

3.1 Algorithm for polyconvex sets

Let $K = \bigcup_{i=1}^m K_i$ be a polyconvex set with convex components K_i . If only a digital image of K is known, an approximation of K which fulfils the conditions of Theorem 2 can be constructed as follows.

- Let K^n be a digitization of K on a square grid with mesh size $t_n \searrow 0$ ($n \rightarrow \infty$) such that $\rho(K^n, K) \leq ct_n$ where the constant c is independent of n . In case of the *Gauss digitization*, sometimes also called *hit-or-miss digitization* $K^n = K \cap t_n \mathbb{Z}^2$, this implies an additional assumption on the set K , namely that K is topologically regular, i.e. the closure of the interior of K equals K . Otherwise the Hausdorff distance between K and K^n can be arbitrarily large or K^n can even be empty, e.g. if K is a line segment. Whereas for the *outer Jordan digitization* $K^n = \left(K \oplus \left[-\frac{t_n}{2}, \frac{t_n}{2}\right]^2\right) \cap t_n \mathbb{Z}^2$, it holds that $\rho(K, K^n) \leq \sqrt{2}t_n$ by definition.
- The union of pixels K^n can be transformed into a simple but possibly non-convex polygon \overline{K}^n with the help of digital straight segments (DSS). In order to do this the boundary of K^n is traced and divided into several DSS parts which are line segments of maximal length that are close to the boundary. It means that the boundary lies in a neighbourhood of the line segment of radius t_n . The concept of digital straight segments is described in detail e.g. in [17] where an algorithm for their construction is given. The representation of the boundary in terms of digital straight segments is not unique. It may vary depending on the starting point and the orientation of the construction.
- For high resolution of the discretization, each of the finitely many concavity points on the boundary of K will have an associate concave vertex on the boundary of the polygon \overline{K}^n . Because of the construction of the set \overline{K}^n , the distance between these two points is at most $(c+1)t_n$. The polygon \overline{K}^n can be decomposed into finitely many (say, m) convex components \overline{K}_i^n . The decomposition of a non-convex polygon in convex components is a non-trivial problem and the best solution in term of minimizing the number of convex components is not an easy task, see [12]. Anyhow we do not need a minimal convex decomposition, but any algorithm can be used.

- The sets \overline{K}_i^n fulfill the conditions of Proposition 3:
 - The sets \overline{K}_i^n are convex and hence have infinite reach.
 - It holds that

$$\begin{aligned}\rho(\overline{K}_i^n, K_i) &\leq \rho(\overline{K}_i^n, K_i^n) + \rho(K_i^n, K_i) \\ &\leq t_n + ct_n = (c+1)t_n \searrow 0 \text{ as } n \rightarrow \infty.\end{aligned}$$

- The sets \overline{K}_i^n do not fulfill the conditions of Theorem 2 because it is not guaranteed that $K_i \subset \overline{K}_i^n$ for all $i = 1, \dots, m$. Hence, define $\widetilde{K}_i^n = \overline{K}_i^n \oplus B_{(c+1)t_n}(o)$. The set $\widetilde{K}^n = \bigcup_{i=1}^m \widetilde{K}_i^n$ is an approximation of K satisfying the assumptions of Theorem 2:
 - The sets \widetilde{K}_i^n are convex and hence have infinite reach.
 - It holds that $K_i \subset \widetilde{K}_i^n$ because of the dilation in the definition of \widetilde{K}_i^n .
 - It holds that

$$\begin{aligned}\rho(\widetilde{K}_i^n, K_i) &\leq \rho(\widetilde{K}_i^n, \overline{K}_i^n) + \rho(\overline{K}_i^n, K_i^n) + \rho(K_i^n, K_i) \\ &\leq (c+1)t_n + t_n + ct_n = 2(c+1)t_n \searrow 0 \quad \text{as } n \rightarrow \infty.\end{aligned}\quad (13)$$

To summarize, we describe the multigrid convergent algorithm to compute the intrinsic volumes of polyconvex sets step by step.

- Extract the boundary of the black phase in the image. The result consists of several 4-connected sequences of pixels, one sequence per object or hole (collection of white pixels surrounded by black pixels) in the image.
- Compute the digital straight line segments (DSS) along the boundaries. They make up several (possibly non-convex) polygons.
- Find the holes in the figure by finding closed DSS contours which are enclosed by another closed DSS contour.
- Resolve the holes by cutting the outer polygon which has a hole into two parts or more if it has several holes.
- Decompose the polygons into convex components by cutting off convex corners. This method does not yield the minimum number of convex parts but is considerably easier than computing a minimal decomposition.
- Compute the intrinsic volumes of all polygons and apply Proposition 3 to get an approximation for the intrinsic volumes of K .
- In order to apply Theorem 2, dilate the convex polygons by a ball whose radius depends on the chosen digitization model but is independent of K .

- Compute the intrinsic volumes of all dilated polygons. The area of a dilated polygon can be computed by Steiner's formula (1), the boundary length of a dilated polygon is given by the boundary length of the polygon plus the perimeter of a circle with the dilation radius, and the Euler number does not change. By means of the inclusion-exclusion formula we get an approximation for the intrinsic volumes of K .

3.2 Algorithm for sets with positive reach

If K has positive reach, the algorithm of Section 3.1 cannot be applied directly because the number of convex components in the approximating sequence will grow to infinity, and thus the conditions of Theorem 2 are violated. But by first applying the algorithm of Section 3.1 and then post-processing its results we achieve multigrid convergence for sets with positive reach. We consider only the approximation K^n in the sense of Theorem 2 here. The differences in the case of Proposition 3 are only of notational but not of conceptual nature.

- Let K be a compact set with positive reach and let $\widetilde{K}^n = \bigcup_{i=1}^{m_n} \widetilde{K}_i^n$ be the result of the algorithm described in the previous section. Note that the number of convex components m_n grows to infinity if K has concavities and that \widetilde{K}^n itself might have concave corners.
- Let $0 < \varepsilon < \text{reach}(K)/2$ and define $\widehat{K}^n = (\widetilde{K}^n \oplus B_\varepsilon(o)) \ominus B_\varepsilon(o)$. This means that concave boundary points of \widetilde{K}^n get smoothed, see Figure 4(a) for an example. Hence \widehat{K}^n has positive reach. To be more precise, $\text{reach}(\widehat{K}^n) = \varepsilon$ if $\text{reach}(\widetilde{K}^n) = 0$, and $\text{reach}(\widehat{K}^n) = \text{reach}(\widetilde{K}^n)$ otherwise.
- The following Lemma shows that all conditions of Theorem 2 are fulfilled (with $m = 1$).

Lemma 4. *With the notation above, it holds that*

- $\text{reach}(\widehat{K}^n) \geq \varepsilon$ for all $n \in \mathbb{N}$,
- $K \subset \widehat{K}^n$ for all $n \in \mathbb{N}$,
- $\rho(K, \widehat{K}^n) \rightarrow 0$ as $n \rightarrow \infty$.

Proof. The first two statements are obvious. We only prove that $\rho(K, \widehat{K}^n) \rightarrow 0$. It holds that

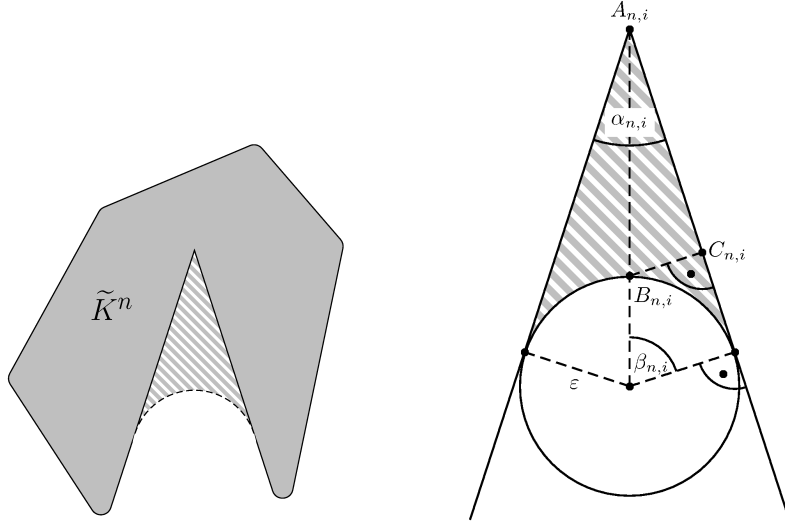
$$\rho(K, \widehat{K}^n) \leq \rho(K, \widetilde{K}^n) + \rho(\widetilde{K}^n, \widehat{K}^n).$$

By (13), we have $\rho(K, \widetilde{K}^n) \rightarrow 0$. Hence, it remains to prove that $\rho(\widetilde{K}^n, \widehat{K}^n) \rightarrow 0$ as $n \rightarrow \infty$. We have $\widetilde{K}^n \subset \widehat{K}^n$ and \widehat{K}^n differs from \widetilde{K}^n only in concave boundary points of \widetilde{K}^n , see Figure 4(a). Hence

$$\rho(\widetilde{K}^n, \widehat{K}^n) = \inf \{r > 0 : \widehat{K}^n \subset \widetilde{K}^n \oplus B_r(o)\} = \max_{\substack{\text{concave} \\ \text{corners } i}} \{d(B_{n,i}, C_{n,i})\}$$

where $d(B_{n,i}, C_{n,i})$ denotes the distance between the points $B_{n,i}$ and $C_{n,i}$, see Figure 4(b). Let $\alpha_{n,i}$ denote the angle in the i -th concavity of the boundary of \widetilde{K}^n and let $\beta_{n,i} = (\pi - \alpha_{n,i})/2$. Then it holds that $d(A_{n,i}, B_{n,i}) = \varepsilon / \cos(\beta_{n,i}) - \varepsilon$ and hence $d(B_{n,i}, C_{n,i}) = \varepsilon(1 - \cos(\beta_{n,i}))$. For increasing n , \widetilde{K}^n does not only converge to K in Hausdorff distance, but also the approximation of the boundary of K by DSS segments gets better. This means that the angles between the linear segments of the boundary of \widetilde{K}^n which correspond to a concavity of K with locally positive reach converge to π for $n \rightarrow \infty$. Hence, $\beta_{n,i} \rightarrow 0$ for all i and therefore $\varepsilon(1 - \cos(\beta_{n,i})) \rightarrow 0$ for all concave boundary points of \widetilde{K}^n . This completes the proof. \square

Applying Theorem 2 we get $V_j(\widehat{K}^n) \rightarrow V_j(K)$ for $n \rightarrow \infty$.



(a) Example of a polygon \widetilde{K}^n (shaded in grey). Compared to \widehat{K}^n , \widetilde{K}^n contains additionally the grey hatched part.

(b) This figure illustrates the definition of the angles $\alpha_{n,i}$ and $\beta_{n,i}$ as well as the points $A_{n,i}$, $B_{n,i}$, and $C_{n,i}$.

Figure 4: Example for the set \widetilde{K}^n and the construction of the set \widehat{K}^n .

- In \mathbb{R}^2 , $V_j(\widehat{K}^n)$ can be computed with the help of \widetilde{K}^n and some geometry. Figure 4(b) illustrates the differences between \widetilde{K}^n and \widehat{K}^n in a concave boundary point of \widetilde{K}^n . The intrinsic volumes of \widehat{K}^n can be computed as follows:

– The Euler characteristic does not change, i.e.

$$V_0(\widehat{K}^n) = V_0(\widetilde{K}^n) \quad (14)$$

- because the dilation / erosion radius to smooth the concavity of \widetilde{K}^n is small.
- The boundary length of \widehat{K}^n is smaller than the boundary length of \widetilde{K}^n . It holds that

$$V_1(\widehat{K}^n) = V_1(\widetilde{K}^n) - \varepsilon \sum_{\substack{\text{concave} \\ \text{corners } i}} (\tan(\beta_{n,i}) - \beta_{n,i}). \quad (15)$$

- The area of \widehat{K}^n is greater than the area of \widetilde{K}^n , because the grey hatched parts in Figure 4(b) are added, i.e.

$$V_2(\widehat{K}^n) = V_2(\widetilde{K}^n) + \varepsilon^2 \sum_{\substack{\text{concave} \\ \text{corners } i}} (\tan(\beta_{n,i}) - \beta_{n,i}), \quad (16)$$

To summarize, we first apply the algorithm of Section 3.1 to get $V_j(\widetilde{K}^n)$ and then compute $V_j(\widehat{K}^n)$ using the correction terms given in (15) and (16). This enables the multigrid convergent computation of $V_j(K)$, $j = 0, 1, 2$, for sets K with positive reach.

3.3 Algorithm for \mathcal{U}_{PR} -sets

The approach to compute the intrinsic volumes of a general \mathcal{U}_{PR} -set is basically the same as described in Sections 3.1 and 3.2. But the difficulty in dealing with \mathcal{U}_{PR} -sets K is that two kinds of concavities might occur, those with (local) reach zero and those with (locally) positive reach. In the following, we show how to distinguish the two types of concavities of K if only the digitization K^n is known.

- Let K be a \mathcal{U}_{PR} -set and let $\widetilde{K}^n = \bigcup_{i=1}^{m_n} \widetilde{K}_i^n$ be the result of the algorithm in Section 3.1.
- Denote the outer (with respect to \widetilde{K}^n) angle of the i -th concavity point on the boundary of \widetilde{K}^n by $\alpha_{n,i}$ (see Figure 4(b)) and let $0 \leq \gamma \leq \pi$.
- If $\alpha_{n,i} \leq \pi - \gamma$, we assume that the current point on the boundary of \widetilde{K}^n corresponds to a boundary point of K which has local reach zero. Therefore this point of \widetilde{K}^n will not be smoothed.
- If $\pi - \gamma < \alpha_{n,i} < \pi$, we assume that the current point on the boundary of \widetilde{K}^n corresponds to a point on the boundary of K with (locally) positive reach. We smooth this boundary point of \widetilde{K}^n as described in the previous section. For each concave boundary point of \widetilde{K}^n we can decide separately if it is smoothed or not because the dilation of \widetilde{K}^n is not carried out in practice. Instead, the effects of this dilation on the intrinsic volumes are computed with the help of (14)–(16).
- Note that $\alpha_{n,i} \geq \pi$ cannot occur because \widetilde{K}^n consists of dilated polygons and hence doesn't have convex vertices.

Of course, for fixed resolution, there are many examples for sets where the above heuristic goes wrong. But for concave boundary points of K with locally positive reach the angles $\alpha_{n,i}$ converge to π for $n \rightarrow \infty$. Hence, for increasing resolution, concavities of K with locally positive reach can be distinguished from those with local reach zero.

Remark 5. All three slightly different versions of the algorithm to construct an approximation of K and compute its intrinsic volumes given in this and the previous two sections can be combined into one depending on the parameter γ .

- If it is known or assumed that K is polyconvex, choose $\gamma = 0$. No concavity points on the boundary of \widetilde{K}^n will be smoothed.
- If it is known or assumed that K has positive reach, choose $\gamma = \pi$. All concave boundary points of \widetilde{K}^n will be smoothed.
- If it is known that K is truly a \mathcal{U}_{PR} -set (i.e. it has reach zero but is not polyconvex) or if nothing can be assumed about the shape of K and therefore the most general case has to be taken, choose some $0 < \gamma < \pi$. In our experiments, $\gamma = 0.01$ turned out to be a reasonable choice. Depending on γ , a concavity point on the boundary of \widetilde{K}^n will possibly be smoothed.

4 Numerical results

In this section we give numerical results for various two-dimensional test cases and provide diagrams showing the convergence of our method in comparison to other methods. The test cases are grouped into

- *convex test sets*: disc, square, square rotated by $\pi/8$, square rotated by $\pi/4$, see Figure 5(a),
- *polyconvex test sets*: L-shape, intersecting discs, frame, touching discs, see Figure 5(b),
- *test sets with positive reach*: halfmoon, ring, see Figure 5(c),
- *\mathcal{U}_{PR} test sets*: butterfly, infinity, see Figure 5(d).

The radius of the circular figures and the sidelength of the rectangular figures, respectively, is fixed to one and the resolution t_n^{-1} ranges from 10 to the maximum possible (about 3,000 to 4,000, depending on the test set) with 4GB of RAM.

For all test cases the Euler characteristic $V_0(K)$ is computed without error. However, if the set K has very small holes with incircle radius less than $2t_n$, the holes are not present in the approximating set K^n and therefore the Euler characteristic is not computed exactly. As far as we know, other algorithms to compute the Euler characteristic have similar problems with very small holes, so it is reasonable to say that the resolution of the image is not good enough in these cases.

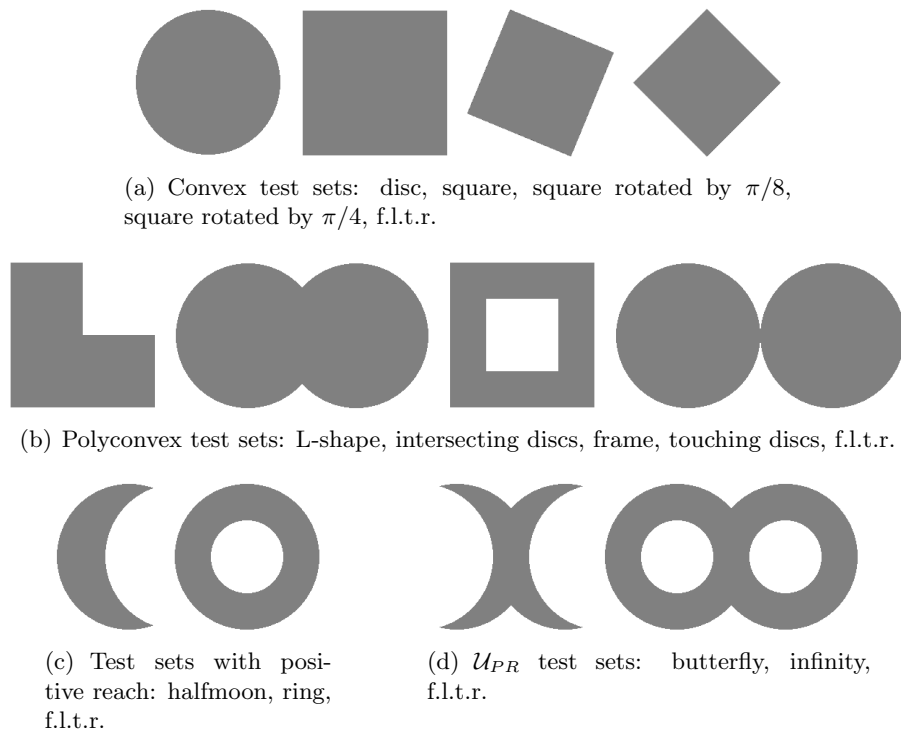
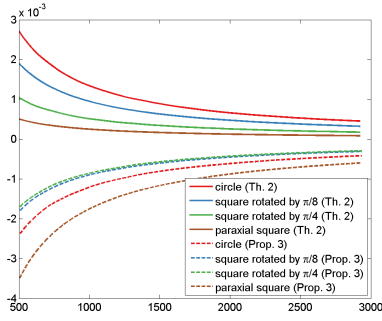
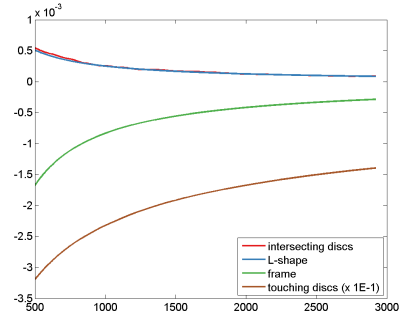


Figure 5: Test sets

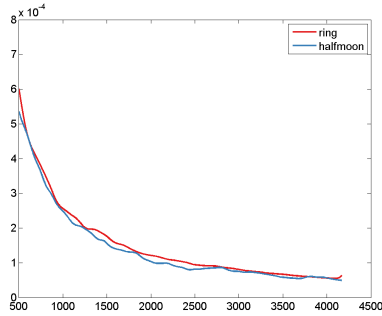
The results for the boundary length depend on the chosen variant of the algorithm, i.e. the variant based on Theorem 2 and the one based on Proposition 3, respectively. This is exemplified in Figure 6(a). We plotted the moving average of 21 values, i.e. for each resolution t_n^{-1} , the mean of the relative errors at resolutions ranging from $t_n^{-1} - 10$ up to $t_n^{-1} + 10$ is shown instead of the relative error at the resolution t_n^{-1} . The solid (dashed) lines show the relative errors of V_1 for the algorithm based on Theorem 2 (Proposition 3). For all four convex test sets the computed boundary length is too large for the first variant (solid lines) because the original set K is a subset of the approximation K^n and the intrinsic volumes are monotone on the family of convex sets. But for the second variant (dashed lines) the dilation step in Section 3.1 can be omitted because it is not necessary that $K_i \subset K_i^n$ (see Section 2.1). This results in underestimated boundary lengths for the convex test sets. For other test sets the results for both variants of the algorithm are of the same magnitude, hence we show only the results for the algorithm based on Theorem 2. The approximation of the boundary length of touching discs is considerably too small, see Figure 6(b)). This is due to the fact that the sharp peaks of the complement the two discs are always cut off when creating DSS segments. For test sets with positive reach and for \mathcal{U}_{PR} -sets the boundary length is approximated very well as can be seen in Figures 6(c) and 6(d). Compared to the widely used method by Ohser / Mücklich in [20], our approach has a larger error for some test sets with small discretization resolutions, see Figure 7(a). But since our algorithm is multigrid



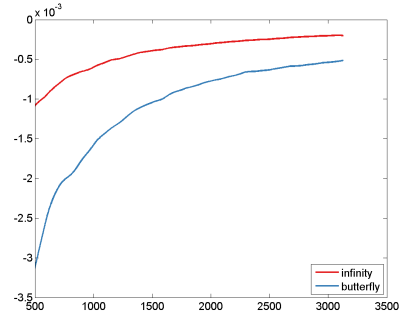
(a) Relative error of V_1 vs. resolution for convex test sets (moving average of 21 values).



(b) Relative error of V_1 vs. resolution for polyconvex test sets (moving average of 21 values).



(c) Relative error of V_1 vs. resolution for test sets with positive reach (moving average of 21 values).



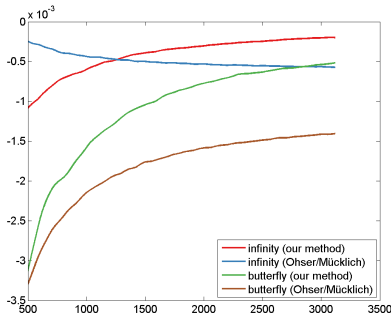
(d) Relative error of V_1 vs. resolution for \mathcal{U}_{PR} test sets (moving average of 21 values).

Figure 6: Comparison of relative errors of V_1 for various test sets.

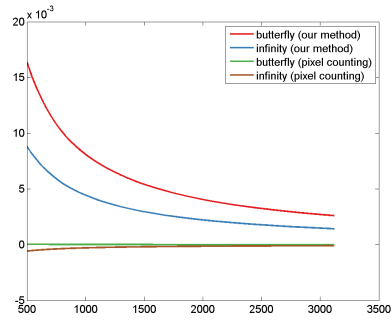
convergent, this changes as the resolution increases.

The area functional computed by the algorithm attains excessively large values for all test images. This is exactly what one expects because the set K is approximated from outside. Anyhow, the focus of this work is to estimate the lower dimensional intrinsic volumes multigrid convergently, as the area can easily be estimated by counting the number of black pixels in an image. See Figure 7(b) for a comparison of errors of V_2 for the \mathcal{U}_{PR} test cases.

In all figures it can be seen that the error of the approximation decreases (in absolute value) as the resolution increases. Furthermore, the results in the \mathcal{U}_{PR} test cases do hardly change for different choices of the parameters γ (the angle threshold) and ε (the smoothing radius). We propose to choose $\gamma = 0.01$ and $\varepsilon = 0.1$ which leads to good results for the test sets in Figure 5. However, ε has to be chosen with respect to the condition $\varepsilon < \text{reach}(K)/2$, see Section 3.2.



(a) Comparison of errors of V_1 of the method by Ohser / Mücklich (see [20]) and our approach (moving average of 21 values).



(b) Comparison of errors of V_2 by pixel counting and our method (moving average of 21 values).

Figure 7: Comparison of relative errors of V_1 and V_2 for \mathcal{U}_{PR} -sets with two algorithms.

5 Summary and conclusions

We proposed an algorithm to estimate all intrinsic volumes for a \mathcal{U}_{PR} -set K and proved that it is multigrid convergent. It is based on a polygonal approximation of the set K which is constructed out of a digital image of K . The proof of multigrid convergence holds in any dimension but so far the algorithm is only implemented in 2D. The problem in higher dimensions is to find an approximation of the set K which fulfils all conditions of Theorem 2 or Proposition 3 and is easy to handle. The algorithm can also be applied to compute the specific intrinsic volumes of Boolean models or other random sets whose realizations in a bounded observation window are almost surely \mathcal{U}_{PR} -sets. Then an edge correction like plus-sampling or the associated point rule has to be applied, see Chapter 2 in [1] for an overview. The method of approximating the unknown set K could also be used to make estimators for tensor-valued Minkowski functionals multigrid convergent. We will not go into details here; see [10] and references therein for an introduction into the theory of Minkowski tensors and [2] for an application to spiral galaxy data.

Acknowledgements

We would like to thank Jürgen Kampf for the present proof of Lemma 1 which is more elegant than the original proof by the authors. Furthermore, we are grateful to thank Markus Kiderlen, Ilya Molchanov and Jan Rataj for fruitful discussions.

References

- [1] O. Barndorff-Nielsen, W. Kendall, and M.N.M. Lieshout. *Stochastic Geometry*, volume 80 of *Monographs on Statistics and Applied Probability*. Chapman & Hall, Boca Raton, 1999.

- [2] C. Beisbart, R. Dahlke, K. Mecke, and H. Wagner. Vector- and tensor-valued descriptors for spatial patterns. In K. Mecke and D. Stoyan, editors, *Morphology of Condensed Matter*, volume 600 of *Lecture Notes in Physics*, pages 238–260. Springer, Berlin, 2002.
- [3] H. Böhm, T. Fischer, D. Riosk, S. Britsch, and M. Reiser. Application of the Minkowski-functionals for automated pattern classification of breast parenchyma depicted by digital mammography. In M. Giger and N. Karssemeijer, editors, *Medical Imaging 2008: Computer-Aided Diagnosis*, volume 6915 of *SPIE proceedings*, 2008.
- [4] D. Coeurjolly, F. Flin, O. Teytaud, and L. Tougne. Multigrid convergence and surface area estimation. In T. Asano, R. Klette, and C. Ronse, editors, *Geometry, Morphology and Computational Imaging*, volume 2616 of *Lecture Notes in Computer Science*, pages 101–119. Springer, Berlin, 2003.
- [5] H. Federer. Curvature measures. *Transactions of the American Mathematical Society*, 93:418–491, 1959.
- [6] H. Federer. *Geometric Measure Theory*. Classics in Mathematics. Springer, Berlin, 1996.
- [7] Carl Friedrich Gauss. *Theorematibus Arithmetici: Demonstratio Nova*, volume II of *Carl Friedrich Gauss: Werke*. Königliche Gesellschaft der Wissenschaften, Göttingen, 1863. (in Latin and German).
- [8] R. Guderlei, S. Klenk, J. Mayer, V. Schmidt, and E. Spodarev. Algorithms for the computation of Minkowski functionals of deterministic and random polyconvex sets. *Image and Vision Computing*, 25:464–474, 2007.
- [9] L. Helfen, T. Baumbach, J. Ohser, and K. Schladitz. Determination of structural properties of light materials. *Imaging & Microscopy*, 4:55–57, 2003.
- [10] D. Hug, R. Schneider, and R. Schuster. Integral geometry of tensor valuations. *Advances in Applied Mathematics*, 41(4):482–509, 2008.
- [11] J. Kampf. On weighted parallel volumes. *Beiträge zur Algebra und Geometrie*, 50:495–519, 2009.
- [12] M. Keil and J. Snoeyink. On the time bound for convex decomposition of simple polygons. *International Journal of Computational Geometry & Applications*, 12(3):181–192, 2002.
- [13] M. Kerscher, J. Schmalzing, J. Retzlaff, S. Borgani, T. Buchert, S. Gottlöber, V. Müller, M. Plionis, and H. Wagner. Minkowski functionals of Abell/ACO clusters. *Monthly Notices of the Royal Astronomical Society*, 284:73–84, 1997.

- [14] M. Kiderlen. Estimating the Euler characteristic of a planar set from a digital image. *Journal of Visual Communication and Image Representation*, 17:1237–1255, 2006.
- [15] M. Kiderlen and D. Meschenmoser. Error bounds for surface area estimators based on Crofton’s formula. *Image Analysis and Stereology*, 28:165–177, 2009.
- [16] S. Klenk, V. Schmidt, and E. Spodarev. A new algorithmic approach to the computation of Minkowski functionals of polyconvex sets. *Computational Geometry: Theory and Applications*, 34:127–148, 2006.
- [17] R. Klette, V. Kovalevsky, and B. Yip. Length estimation of digital curves. In *Vision Geometry VIII*, pages 117–129, 1999.
- [18] R. Klette and A. Rosenfeld. *Digital Geometry*. Morgan Kaufmann, San Francisco, 2004.
- [19] T. Mrkvička and J. Rataj. On the estimation of intrinsic volume densities of stationary random closed sets. *Stochastic Processes and Applications*, 118(2):213–231, 2008.
- [20] J. Ohser and F. Mücklich. *Statistical Analysis of Microstructures in Material Science*. John Wiley & Sons, Chichester, 2000.
- [21] J. Ohser, W. Nagel, and K. Schladitz. Miles formulae for Boolean models observed on lattices. *Image Analysis & Stereology*, 28:77–92, 2009.
- [22] J. Ohser and K. Schladitz. *3D Images of Materials Structures: Processing and Analysis*. Viley-VCH, Weinheim, 2009.
- [23] R. Schneider and W. Weil. *Stochastic and Integral Geometry*. Springer, Berlin, 2008.
- [24] E. Spodarev and V. Schmidt. On the local connectivity number of stationary random closed sets. In C. Ronse, L. Najman, and E. Decenciere, editors, *Mathematical Morphology: 40 Years On. Proceedings of the 7th International Symposium on Mathematical Morphology*, Springer Series: Computational Imaging and Vision, pages 343–354, 2005.
- [25] R.A. Vitale. The Wills functional and Gaussian processes. *The Annals Of Probability*, 24:2172–2178, 1996.
- [26] J.M. Wills. Zur Gitterpunktanzahl konvexer Mengen. *Elemente der Mathematik*, 28:57–63, 1973.